AD-A139 799 BEHAVIOR OF CASCADED AIRFOILS UNDER CONDITIONS OF HIGH MEAN LOADING AND F.. (U) STEVENS INST OF TECH HOBOKEN N J DEPT OF MECHANICAL ENGINEERI.. F SISTO ET AL. 1/1

UNCLASSIFIED 15 DEC 83 ME-RT-83007 N00014-82-K-0369 F/G 21/5 NL

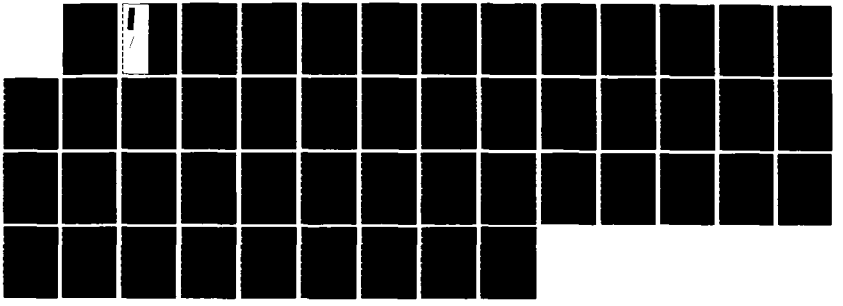

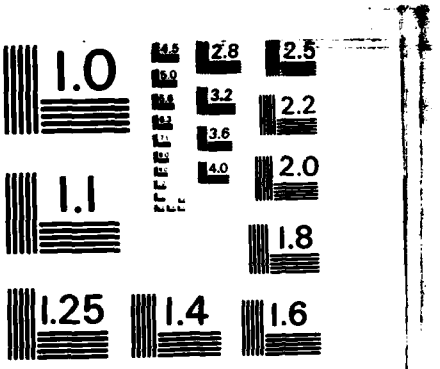

STEVENS INSTITUTE
OF TECHNOLOGY

CASTLE POINT STATION
HOBOKEN, NEW JERSEY 07030

DEPARTMENT OF MECHANICAL ENGINEERING

BEHAVIOR OF CASCADED AIRFOILS UNDER CONDITIONS OF HIGH MEAN LOADING AND FLOW UNSTEADINESS

F. Sisto
and
R.B. Cole

15 December 1983

Final Technical Report
under
Contract N00014-82-K-0369, NR094-419
for
The Period: 1 June 1982 to 31 May 198

Approved for Public Release
Distribution Unlimited

Prepared for:

Office of Naval Research
800 N. Quincy Street
Arlington, VA 22217

Stevens Institute of Technology Castle Point, Hoboken, New Jersey 07030
Department of Mechanical Engineering
201·420·5592

The enclosed Final Report under Contract N00014-82-K-0369 being distributed according to the following list:

Addressee	DODAAD Code	Number of Copies
Scientific Officers		
• Associate Director for Engineering Sciences, Materials Division Office of Naval Research 800 North Quincy Street Arlington, VA 22217	N00014	1
• Dr. Gerhard Heiche Naval Air Systems Command Department of the Navy Washington, D.C. 20361	AIR-310	1
• Mr. George Derderian Naval Air Systems Command Department of the Navy Washington, D.C. 20361	AIR-310E	1
• Office of Naval Research Resident Representative-New York 715 Broadway, 5th floor New York, NY 10003	N62927	1
• Director, Naval Research Laboratory, ATTN: Code 2627 Washington, D.C. 20375	N00173	6
• Defense Technical Information Center Bldg. 5, Cameron Station Alexandria, Virginia 22314	S47031	12
• Office of Naval Research 800 N. Quincy Street Arlington, VA 22217	N62879	1
• Professor M.F. Platzer, Chrmn. Department of Aeronautics Naval Postgraduate School Monterey, CA 93940	-	1
• Professor R.P. Shreeve, Director Turbopropulsion Laboratory Naval Postgraduate School Monterey, CA 93940	-	1

F. Sisto
Principal Investigator

BEHAVIOR OF CASCADED AIRFOILS UNDER CONDITIONS OF HIGH MEAN LOADING AND FLOW UNSTEADINESS

by

Fred Sisto
Richard B. Cole

Mechanical Engineering Department
Stevens Institute of Technology

Final Technical Report

Prepared for

Office of Naval Research
800 North Quincy Street
Arlington, Virginia 22217

Contract No. N00014-82-K-0369
Work Unit No. NR094-419

December 1983

ABSTRACT

A compressor designed for LDA measurement of unsteady rotor flow has been constructed. A blower in series uncouples throughflow and compressor speed providing wide variability of load. LDA data acquisition and processing systems have been designed and partially completed. Candidate data processing algorithms have been studied. Propagating stall has been detected experimentally but no LDA data have been obtained defining unsteady velocities.

Modelling of a cascade with doubly periodic flow has been initiated. Solutions with nonuniform loading have been demonstrated; future addition of the vortical flow downstream should lead to an instability criterion and the subsequent development of time dependence.

Unsatisfactory progress has prompted project reorientation with a CFD cascade model which creates and convects vortex "blobs" according to the Random Vortex Method. This model may be merged with the previous analytical model of nonuniformly loaded cascades.

Compressor/LDA development will continue with emphasis shifting to a windtunnel experiment with one stalling airfoil. Measured flow periodicity will validate the CFD model and allow application to cascades. This objective with 3D application will allow predicting the stall zone number in compressors, the missing datum in assessing blade resonance with stall frequency. The tangential wavelength is also key to predicting stall flutter.

TABLE OF CONTENTS

Page

Title Page.....i

Abstract.....ii

Table of Contents.....iii

I. Introduction and Background.....1

II. Instrumentation System

Laser Doppler Anemometer and Data.....4

Acquisition System.....13

LDA Data Processing.....18

III. Analytical/CFD Model of Cascades.....27

IV. Research Compressor.....35

V. Conclusions.....38

References.....41

DD Form 1473.....42

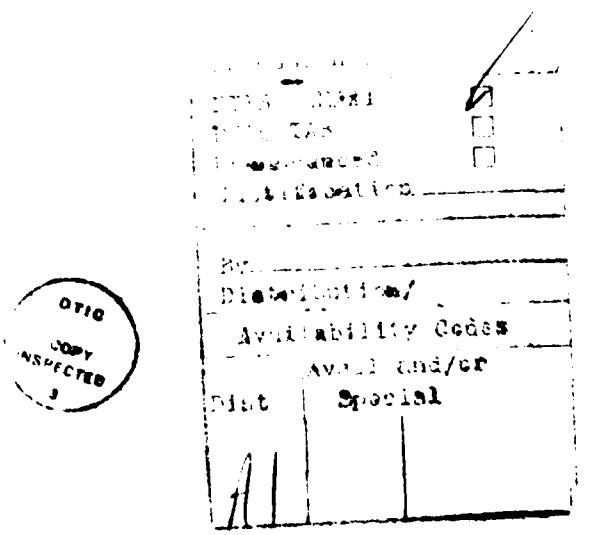

INTRODUCTION AND BACKGROUND

The axial-flow compressor and fan components of aircraft gas turbine engines are typically designed for minimum weight and high efficiency. In the aircraft application frequent operations at off-design conditions are required, resulting in the occurence of potentially dangerous stall, or near stall, in these compression components. The danger is related to the possibility of vibration, fatigue and eventual failure of the axial-flow blading. These vibrations may be self-excited in which case they are termed "stalling flutter", or else they may result from a resonance with the frequency of stall encounter in the "stall propagation" mode. Hence the detailed mechanism of blade stall in a cascade of airfoils needs further definition. Present understanding is deficient in many respects.

Deficiencies with respect to stall propagation relate mainly to the frequency of stall encounter by a blade. Although the propagation rate of a stall patch along the cascade may be predicted quite accurately, the number of such patches in the flow annulus (i.e. wavelength along the cascade) cannot presently be predicted. Hence the product of rate and wavelength which determines the forcing frequency is not accessible to the design process.

The deficiency with respect to stalling flutter is even more severe; neither the precise onset of the phenomenon nor its severity can be predicted from first principles. It is known to

be related to operation at high incidence, in the proximity of stall, and periodic stalling and unstalling is thought to take place during each cycle of oscillation. Recently compressibility phenomena have been implicated in the stalling process in certain instances.

As an overall statement it seems clear that a better definition is needed of how a cascaded airfoil stalls dynamically. Consequently, the research program reported here has had as its primary objective the detailed measurement of the velocity field in a compressor rotor passage. It is clear that this is an unsteady velocity under the condition of interest. Furthermore, the highest positive incidence is usually obtained on the first rotor row of blades, hence stalling flutter and instigation of propagation stall may be studied, initially, in a single stage compressor. Multistaging, moving shockwaves, and other effects can be left to future consideration.

With this background the basic thrust of the research was intended to be experimental. A research compressor, specifically conceived for this purpose, was designed and built. A laser doppler anemometer was converted to the service of these turbomachinery measurements, and a data acquisition, storage and processing system was procured. These efforts are detailed in the following sections.

Finally, in anticipation of obtaining a complete velocity mapping of a rotor passage in three dimensions and time, a preliminary modelling of the flow was begun in order to help to

guide later experiments and assess the difficulty of the desired analytical description.

Many of the preliminary phases of the research were reported in [1], the final technical report for the previous contract in which this work was initiated.

LASER-DOPPLER-ANEMOMETER (LDA) MEASUREMENT AND DATA-ACQUISITION SYSTEM

LDA Measurement

Efforts were directed both at installing the LDA apparatus in conjunction with the compressor test-rig and at developing the LDA technique itself.

LDA Mounting on Compressor Test Rig

The compressor rig was modified and added to in order to allow installation of the LDA for velocity measurements.

To allow optical access to the flow passages of the compressor, a 2" x 3 1/2" window was designed and installed on the compressor rig. The final window design involved 1/16"-thick Plexiglas material cemented to a window holder. The window holder formed and held the window material in a cylindrical shape matching that of the outside diameter of the compressor-rig's annular flow passage. The window holder mates with one of the compressor rig's housing rings. The holder can be adjusted relative to the housing ring, allowing the window to be flush with the outside diameter of the annular flow passage. The housing ring containing the window can be assembled into the complete compressor rig at a variety of axial stations. This allows LDA access not only to the compressor rotor and blades but also to portions of the annular flow passage at positions either upstream or downstream of the rotor station. Optical calculations and tests with the LDA verified that the window would not significantly alter the optical path

of the LDA beams. The possibility of LDA attenuation due to excessive reflection from the window surfaces was also considered. It was verified that commercial optical coatings are available to minimize such reflection, if necessary.

To provide support and adjustment of the LDA itself, a table was designed and constructed. The table locates the LDA apparatus approximately parallel to the compressor axis, and an adjustable mirror provides redirection of the LDA's optical axis to be transverse to the compressor axis. This arrangement minimizes the possibility of the LDA optics being struck in the event of a compressor blade failure. The design of the LDA table provides for three-dimensional adjustment of the entire LDA assembly. While height adjustment is provided, it is not intended to be used as frequently as LDA position adjustment in a horizontal plane. Horizontal adjustment allows two degrees-of-freedom by way of an adapted milling table. The axes of this table are aligned to provide independent positioning of the LDA in either axial or transverse directions relative to the compressor rig. Sufficient motion is provided to allow use of the entire window in the compressor-rig housing (approx. 2", axial) and to locate the LDA measuring volume at any radial position in the annular flow passage (12" i.d., 20" o.d.). To control vibrations, the LDA table was mounted on concrete pads keyed to the concrete floor of the laboratory. Initial qualification tests for vibration suggested that the LDA table was not subject to significant vibration when the compressor rig was running.

Particle Seeding

Development of the LDA technique primarily involved work concerned with the particle-seeding of the air flow which is required by the technique. Also involved was development of experimental methods and equipment to allow routine calibration and performance checks of the LDA system.

The requisite characteristics of LDA particles and the method of introducing them for use was clarified by calculations. These involved:

(1) modeling response of the particle to unsteady velocities in the surrounding air,

(2) acceleration/deceleration of a particle injected into a moving air stream,

(3) dispersion/dilution of particles during their equilibrium with the surrounding air flow, and

(4) concern for the rate of data acquisition from LDA particles.

(1) LDA Response to Unsteady Air Velocities

For the purposes of estimating response to unsteady air velocities, the LDA particle was modeled as an isolated sphere subject to Stokes-Law drag by a surrounding air stream. It is then possible to estimate the amplitude and phase error in particle response. Under these conditions, the particle response is first-order in velocity with respect to time. Response can, therefore, be characterized in terms of a time constant:

$$\tau = \frac{d^2\rho}{18\mu}$$

where d = diameter of spherical particle

ρ = density of spherical particle

μ = dynamic viscosity of surrounding fluid

As a reasonable baseline, the following parameter values were chosen:

d = 1.0 μm

ρ = 1.0 gm/cm^3 (e.g., water)

μ = 1.81 x 10^{-5} N-s/m2 (e.g., air at STP)

resulting in the calculated value:

τ = 1.25 x 10^{-5}s $\cong$ 10^{-5}s

For such a value of the particle time constant, the relative (velocity) amplitude response, A, and relative phase, $\emptyset$, of the particle's oscillation can be readily expressed in first-order form:

$$A = \{1/[1 + (2\pi f\tau)^2]\}^{1/2}$$

$$\emptyset = \arctan(2\pi f\tau)$$

Amplitude and phase characteristics of the baseline particle are shown in Figure 1(for $\tau = 10^{-5}$ s) along with additional curves. Response curves for particles twice or half as dense as water (τ = 2 x 10^{-5}s, τ = 0.5 x 10^{-5}s; respectively) and for particles of 2 μm and 0.5 μm diamters (τ = 4 x 10^{-5}s, τ = 0.25 x 10^{-5}s; respectively) are included. Similar results, in non-dimensional form are reported in Ref. 2 and are in agreement with the values of Figure 1.

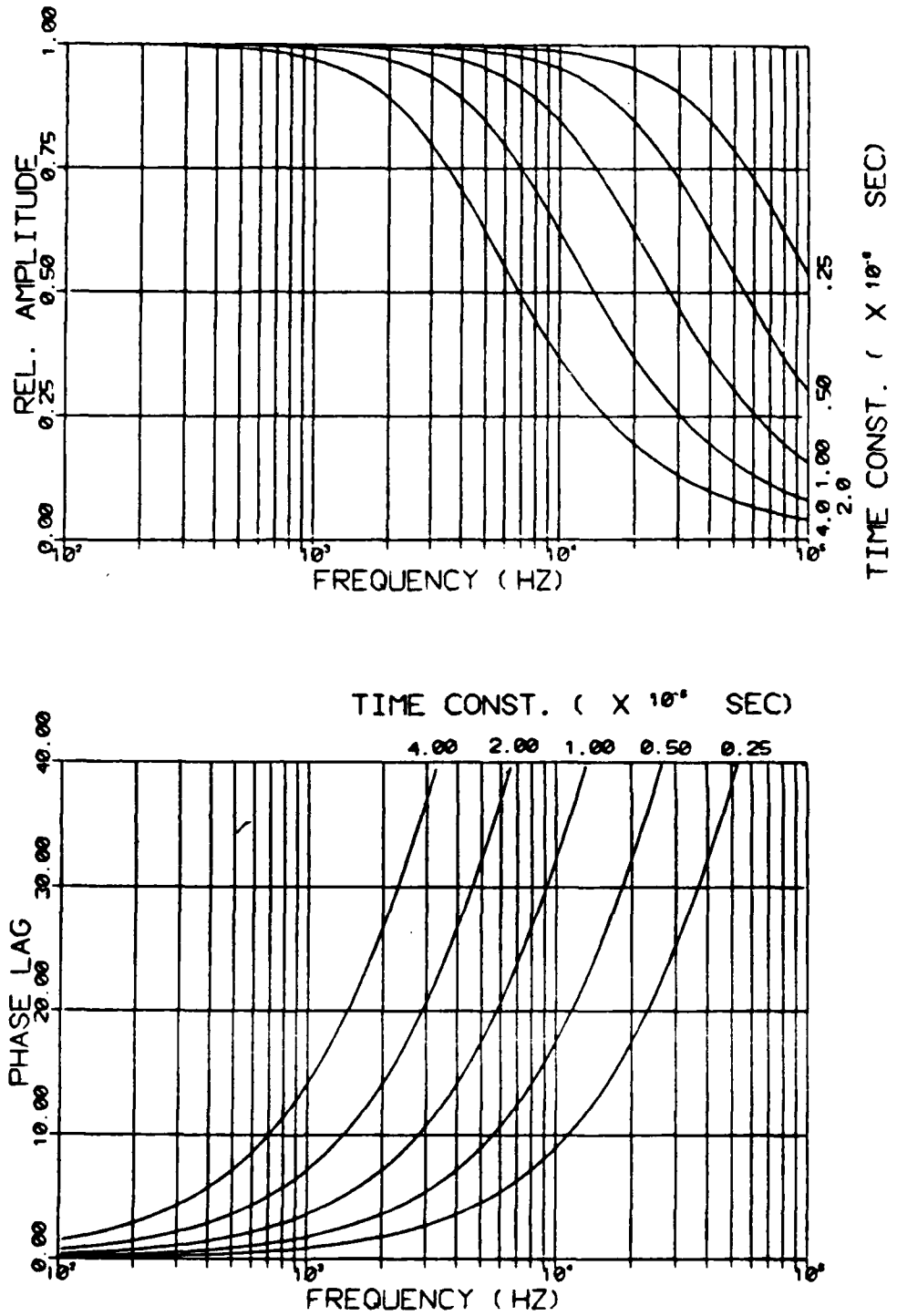

FIGURE 1: Relative Amplitude and Phase Lag (in degrees) Calculated for a Single Particle in Airstream of Sinusoidally Varying Velocity

One concludes from the values of Figure 1 that liquid particle sizes near 1 μm could be expected to respond with sufficiently small error in unsteady velocity up to frequencies of say, 1000 Hz (A = 0.997, ϕ = 4.3 degrees). Unsteady velocity components above such a frequency are not likely to be of major significance in the subject propagating-stall situations. Therefore, such particles are suitable, at least on an unsteady-response basis, for LDA seeding.

(2) Seed-Particle Equilibration Following Injection Into Moving Air Stream

The need to add or "seed" particles into the air flow requires concern for the speed with which the seeded particle equilibrate in velocity with the surrounding air flow. Assuming that Stokes Law of viscous drag applies (Reynolds Number based on relative velocity < 0.5), the relative particle velocity is first-order in time for a single, isolated particle suddenly seeded (injected) into a surrounding air stream.

For the "baseline" situation mentioned above (1. μm water particle in STP air), the distance traveled by such a particle in equilbrating in velocity within 1% can be calculated (Ref. 2) to be only about 3 mm. On this basis, particle acceleration/deceleration allows that particle injection can be at virtually any practical distance upstream of the LDA measuring volume. That is, factors other than simple particle acceleration/deceleration will dominate choice of an appropriate upstream position for seeding.

(3) Carrier-Gas Equilibrium Following Injection

LDA-particle seeding involves injection of particles and, with them, a surrounding carrier-gas (air) flow. For this reason, an additional aspect of particle response involves equilibration of the carrier-gas flow with the main-stream air flow. This situation was modelled as a turbulent-jet-mixing problem in order to estimate the distance of particle (jet) travel required between the injection point and measuring point to insure near-equilibration of velocities.

Jet-mixing theory by Abramovich (Ref. 3) was applied to the problem of calculating the distance downstream of carrier-gas injection at which the carrier-gas (and particle) velocity and the free-stream velocity would be equilibrated within a specified difference. While the unsteady velocities expected in turbomachine tests are probably not well approximated by such a jet-mixing model, the intent of the modelling was to establish whether carrier-gas equilibration was likely to represent a practical problem or not; the jet-mixing approach was thought to provide information as to upper limits on the distances downstream required for equilibration and a basis for judging whether this problem might be practically significant or not.

The results of calculations showed that unless the carrier-gas and (mean)free-stream velocities are well matched at the point of carrier-gas (and particle) injection, large distances downstream are required (e..g, 1000 nozzle diameters) and considerable dilution

and jet spreading (e.g., to tens of nozzle diameters) of the carrier-gas will have occurred by the point where the carrier-gas and free-stream have nearly equilibrated.

It was concluded that particular attention would have to be paid to this factor during experimental development of the seeding technique.

(4) LDA Data Rate

Particularly in light of a possible data-reduction scheme requiring high sampling rates (Ref. 1), possible LDA data rates were estimated in order to check feasibility.

Theoretically, data rate is limited by the fringe spacing in the LDA measuring volume, the counting algorithm employed by the LDA processor, the seed-particle speed (air speed), and the seed-particle concentration. Practically, the nature of the particle (size, shape, material) and the laser-beam intensity also influence actual data rates.

Theoretical limits on data rates are shown in Figure 2 where fringe spacing and particle velocity are shown as determining maximum data rate. The data presented are based on an assumed eight fringe crossings being required for a single measurement. It is clear from the results that a reasonable velocity range may be covered with data rates high enough to allow gated LDA measurements of the sort under consideration for the present work.

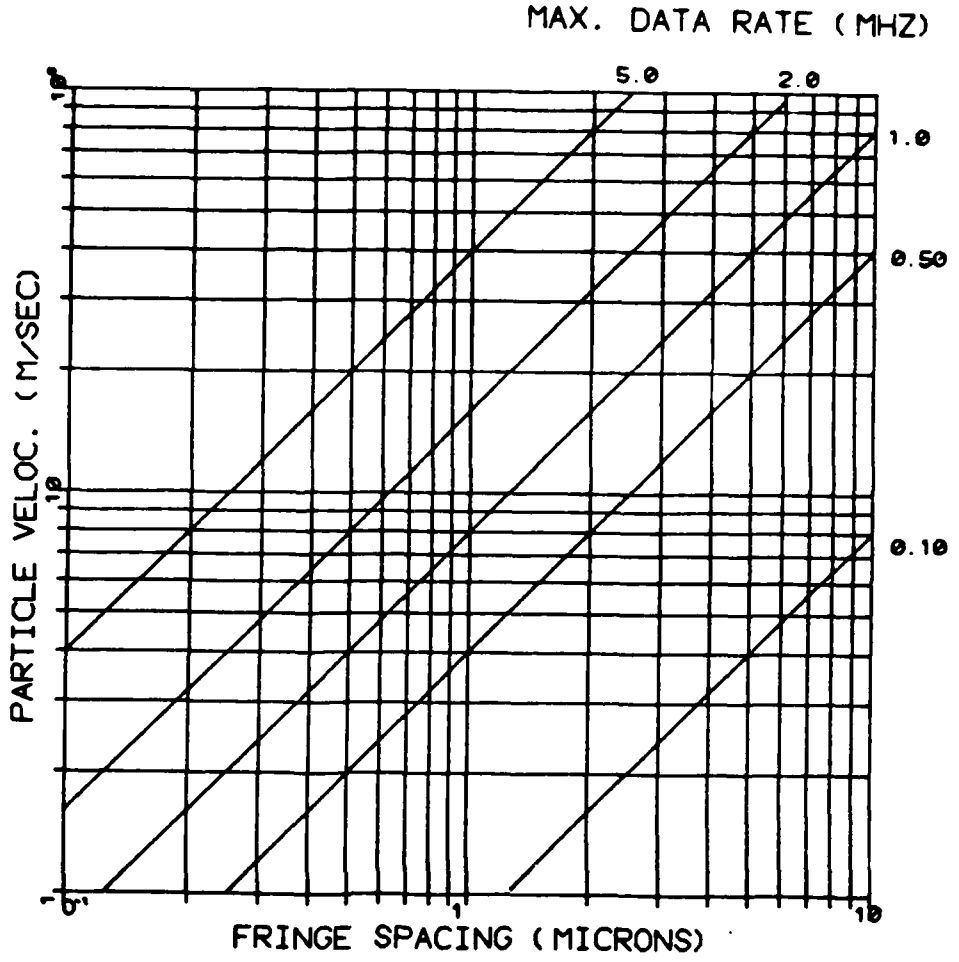

FIGURE 2: Maximum LDA Data Rates for Varying Fringe Spacing and Particle Velocity (Traversal of 8 Fringes for LDA Counter Processor)

Developments to Routinize LDA Use

Many bench-top experiments were carried out in the course of developing the LDA methods. A major portion of these were aimed at providing effective seeding, flow situations, etc. for convenient, effective checks on operation, calibration, etc. of the LDA. The earliest of these experiments typically involved air flows and smoke particles, in anticipation of the need for a somewhat similar method for use with the compressor rig. These were, however, abandoned in favor of latex spheres in water and a water "tunnel" to provide more convenient reproducibility.

LDA Data Acquisition & Storage

Both hardware development and software programming were undertaken during the subject contract period with the aim of providing for gated signals from the LDA. Figure 3 shows schematically the anticipated "sparse-burst" nature of the LDA data to be acquired and stored. The data bursts shown occur during the short "gate-open" periods for which a selected portion of a blade passage is within the measuring volume of the LDA. LDA velocity measurements obtained by the LDA at other times are not of interest and therefore are blanked out during the relatively long gate-closed periods.

To provide for the expected data, the data-acquisition and storage system shown schematically in Figure 4 was designed and construction initiated.

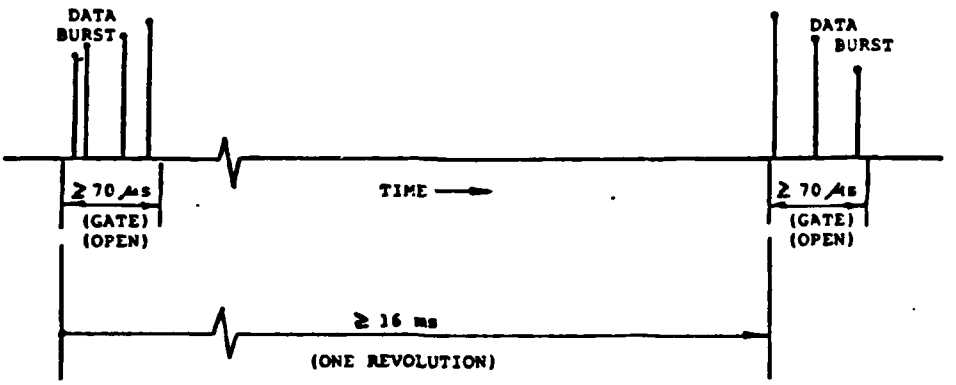

FIGURE 3: Schematic of Expected Data
(In Sparse Bursts)

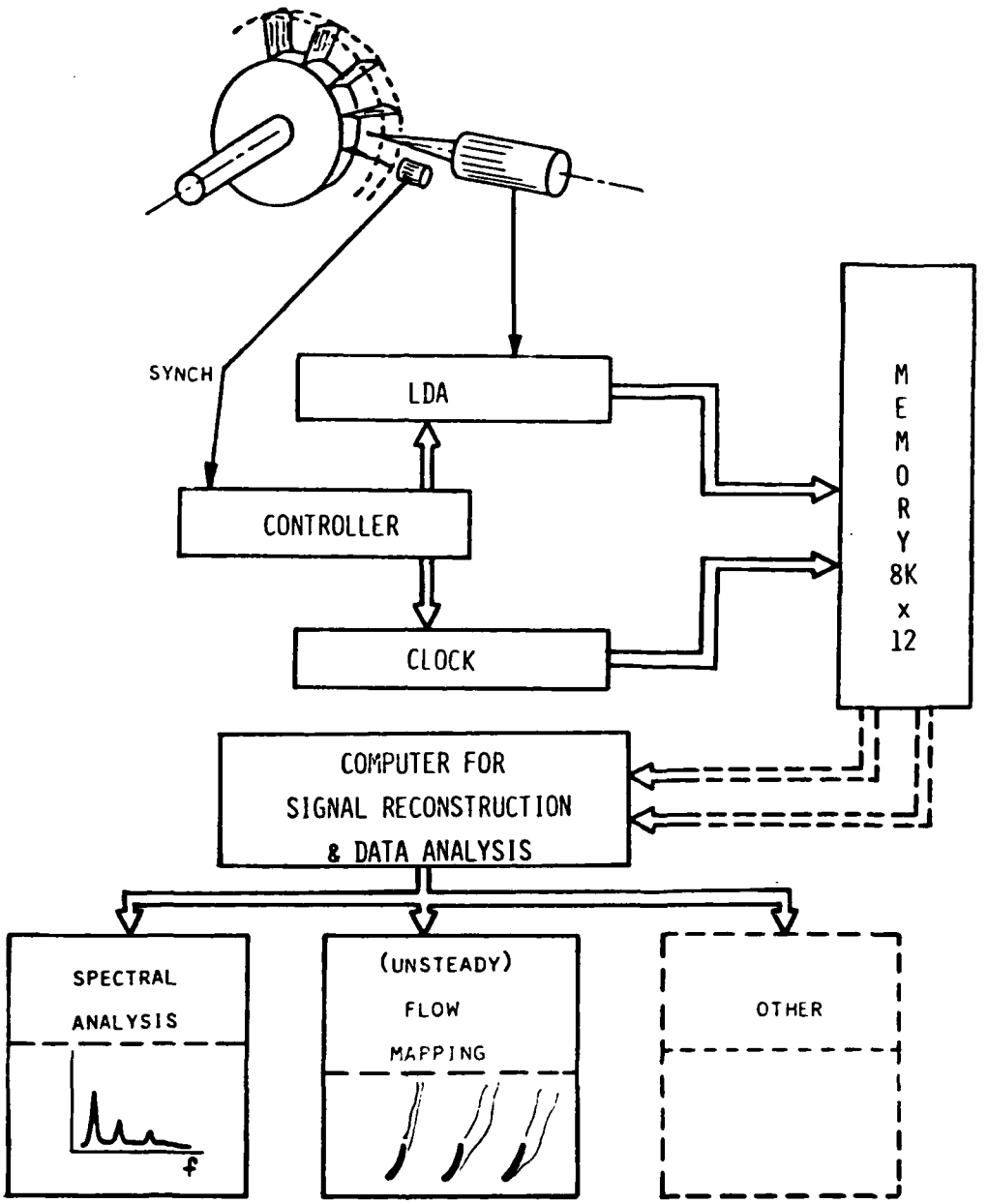

FIGURE 4: Schematic of Data Acquisition and Storage System

The backplane wiring of a card rack for the single-board computer and two additional boards was completed (with checking). One of the additional boards, containing clock and DMA controller was constructed. However, at completion of the contract, the second board containing the serial interface had not yet been contructed.

Programming of the microcomputer to provide for gating of the LDA signal, etc. was started using a microprocessor development system, but this work was not completed.

Figure 5 shows in more detail the functional blocks which comprise the system. To accommodate the high data rates desired, direct memory access (DMA) was provided under the control of a single-board microcomputer based on an Intel 8085A microprocessor. The microprocessor receives once per revolution pulses from a sensor/signal conditioner installed on the compressor test rig. These pulses serve as the basis for the microcomputer to determine at what time the gate should be opened, allowing any data acquired from the LDA to be transmitted and stored in memory. The microprocessor, in turn, signals the DMA controller at the appropriate time, and data from the LDA Counter Processor (f_D, the Doppler frequency, corresponding with measured velocity) begins to flow into the memory of the system. For each 12-bit item of velocity data from the LDA that is stored, a corresponding 12-bit, 100-KHz clock reading is stored to record the time (t) at which the velocity was measured. The clock is effectively read with 24-bit resolution, however, by storing either most- or least-significant sets of 12 bits. Most-significant-bit (MSB) data are stored only when the MSB data are incremented. This is signaled

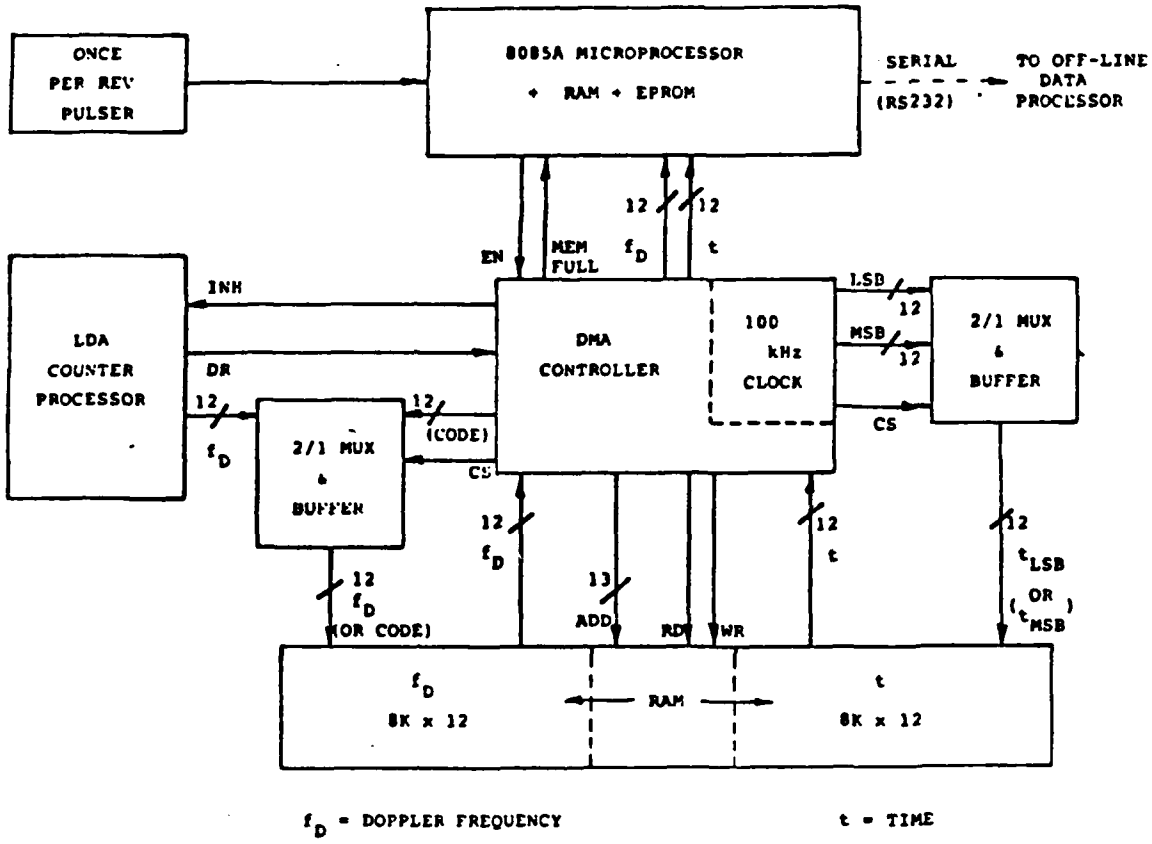

FIGURE 5: Functional Block Diagram of Data Acquisition and Storage System

by a code value appearing in the corresponding Doppler frequency register rather than an actual vlaue of f_D. The 12-bit data are stored in banks of RAM for later recall and processing. Since both LDA output and timing clock data are in coded form, some processing is required merely to retrieve the physically meaningful values from the stored data.

The microcomputer serves to withdraw data from memory via the DMA controller and transmit the data to another data-processing computer. This transmission is designed to be via an RS-232 serial port.

LDA DATA PROCESSING

Numerical simulations were continued with the aim of evaluating alternative schemes for deducing unsteady velocities, power spectra, etc. from the previously described LDA data. The work previously reported (Ref. 1) was extended to determine the feasibility of signal reconstruction for the present application according to the method of Yen (Ref. 4). Interest in this method arose from earlier simulations by other methods (Ref. 1) which indicated numerical difficulties with reconstructing the original signal from the sparse-burst samples of the subject experiment.

Simulations using Yen's Minimum Energy Method

The "minimum energy" method of Yen (Ref. 4) was tested with the hope of finding that it would minimize the tendency observed with other methods to generate large, false peaks or "blips" in the reconstructed signal. These spikes presumably derive from numerical inaccuracies.

Yen's method involves numerically determining a fictitious set of sample values, equally spaced in time that would, upon signal reconstruction, match the actual measured signal values at those arbitrary times at which the actual samples were taken. The matching is subjected to the constraint that the sum of the squares of the sample values of the fictitious set should be a minimum.

Figure 6 shows an example of a mixed frequency signal from which samples were drawn in bursts (see Fig. 3), with two samples randomly timed within each burst or gate-open period. The points shown represent the pairs of samples. Yen's algorithm was then used to reconstruct the signal from these pairs of samples by using the intermediary of the fictitious, uniformly spaced series of samples referred to above.

Figure 7 shows the signal reconstructed from the pairs of randomly spaced samples for an example case of 80 samples (40 pairs). At two times (approx. 29 and 39 time units) large spikes can be seen, and in fact, smaller spikes are apparent in the neighborhood of every pair of samples. All such spikes are apparently the result of numerical errors, probably deriving from inaccuracies in the matrix inversion algorithm used to solve the reconstruction equations. This is evidenced by the fact that the occurrence of these spikes and their magnitudes differed considerably from one matrix-inversion algorithm to another. For example, an early Scientific Subroutine Package (SSP) program was found to give somewhat less trouble than several more-modern International Mathematics and Statistics Library (IMSL) routines for matrix inversion.

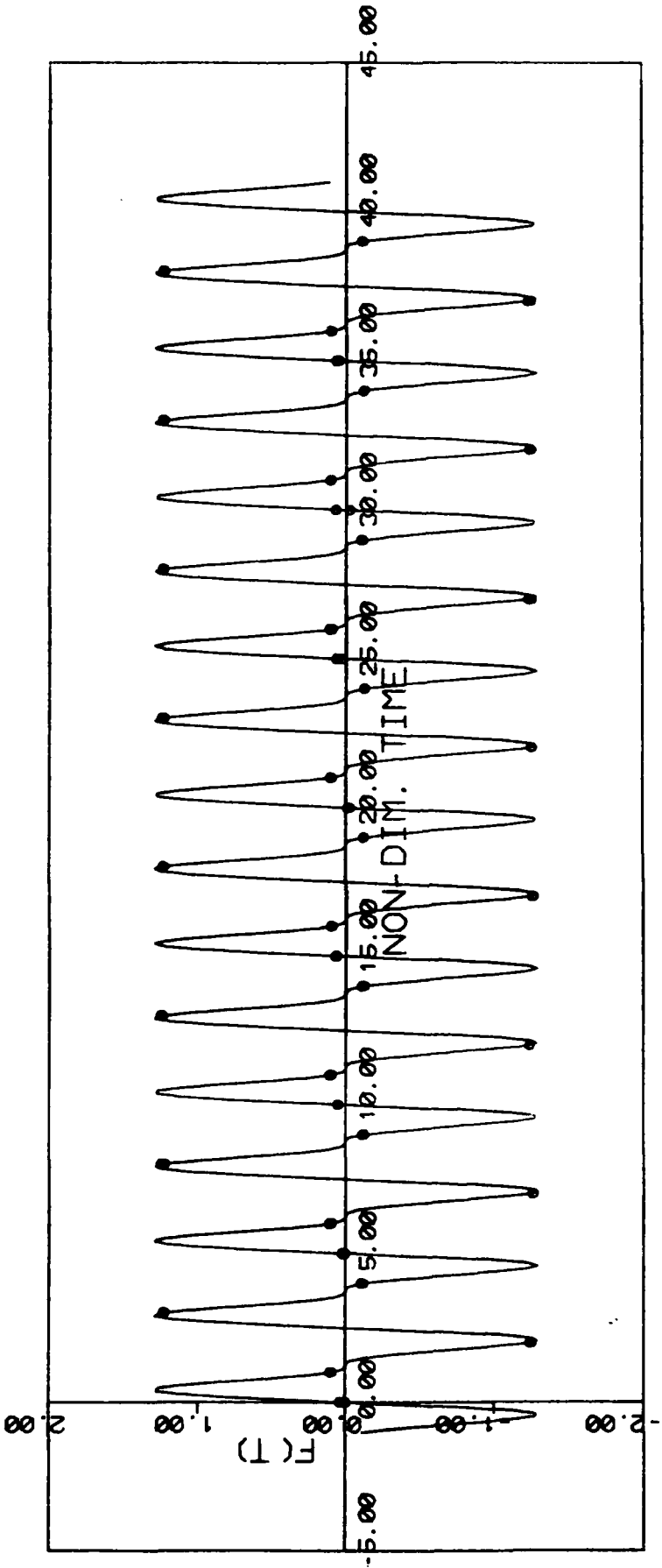

FIGURE 6: Original Mixed-Frequency Signal (Showing Sampling in Bursts of Two)

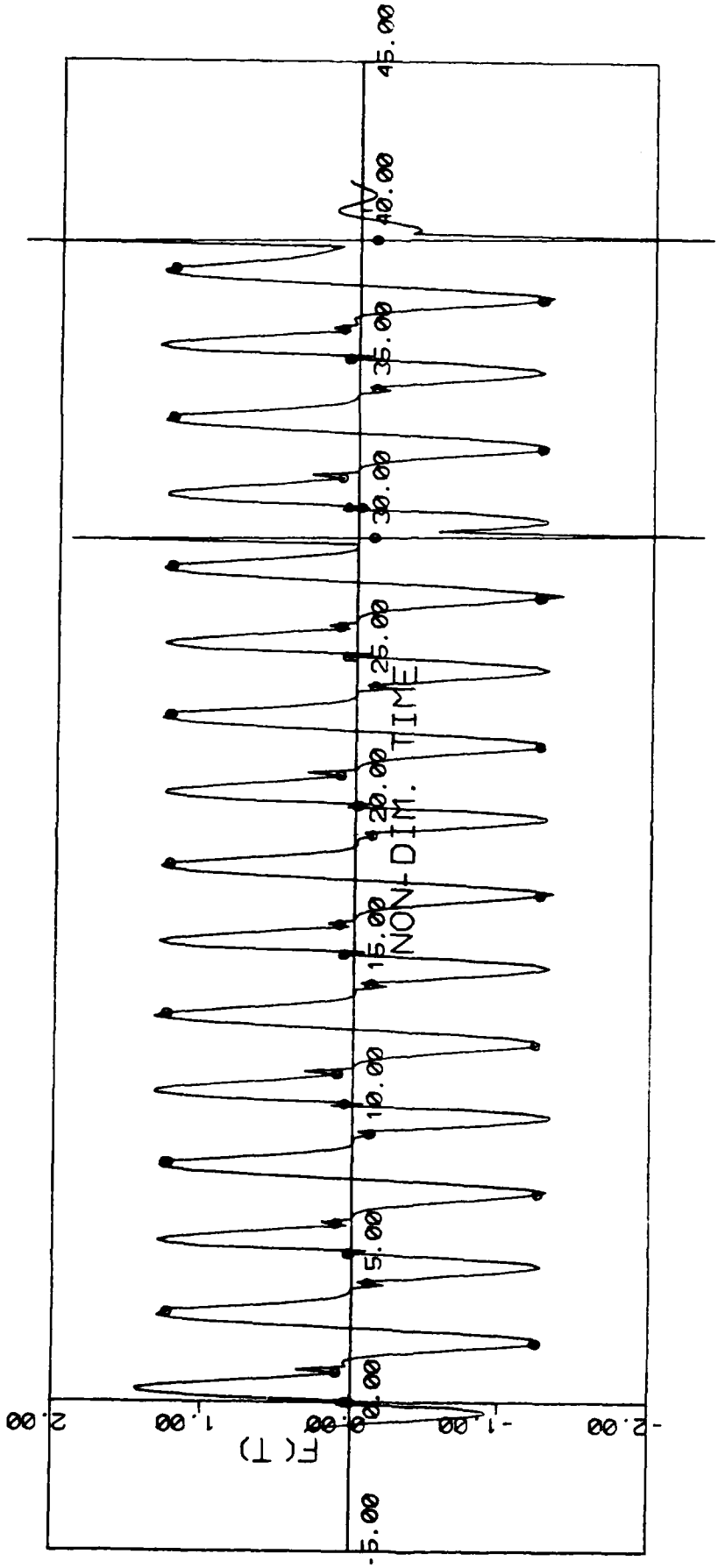

FIGURE 7: Reconstructed Signal (With Paired Samples Shown)

It appears that low-pass filtering of the reconstructed signal could readily eliminate these spikes without interfering appreciably with the much-lower-frequency components which represent the original signal. Figures 8a and 8b show power spectra for the original and the reconstructed signals of Figures 6 and 7. It is clear that the obvious high-frequency spikes of the reconstructed signal do not seriously impede meaningful spectral analysis at the lower frequencies of interest. However, it is notable that in all cases tested, increasing the number of samples always led to increasingly large spikes occuring at larger sample sizes. Thus, there is evidence of an inherent mismatch between the reconstruction method and the drive for increased resolution and signal-to-noise ration via increased sample size.

In cases involving a relatively small number of samples (e.g., 10), spikes were not observable in reconstructed signals and certainly were not troublesome. However, either increasing the number of samples in each burst (during each gate-open period) or increasing the number of gate-open periods led to increasingly large spikes, finally to the point of seriously disrupting the reconstructed signal.

The spikes observed in the reconstructed singals were studied as to their sensitivity to the parameters defining the sampling situation, especially the time duration of the "gate-open" period relative to the duration betwen gate-open periods. At gate-open periods sufficiently large relative to the gating period (e.g. 30%), it was found that the spikes virtually disappeared.

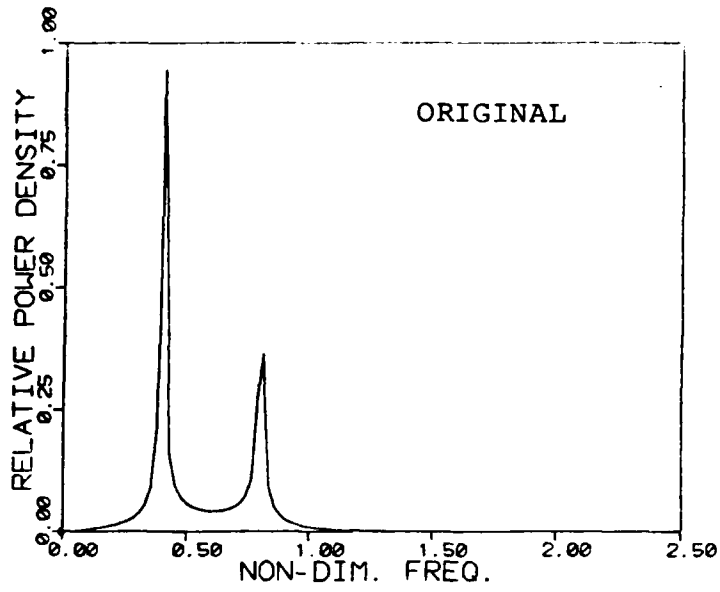

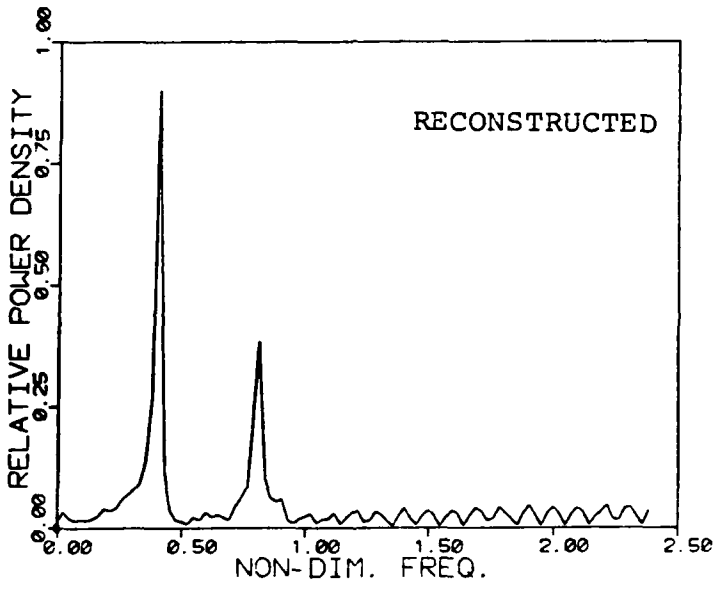

FIGURE 8: Power Spectra for Original and Reconstructed Signals

In light of the numerical difficulties encountered with implementing Yen's method of minimum energy, the typical form of the matrices involved was studied. The algorithm for reconstruction involves inversion of a matrix with elements near unity in value on the diagonal and near the diagonal. Elements of the matrix are much smaller elsewhere (far off-diagonal). This approximately "block diagonal" form with near-zero elements off-diagonal would tend toward a singular matrix of zero determinant in the limit of very narrow gate-open periods with much longer intervening gate-closed periods. It is possible that specialized inversion methods for such block matrices are available. However, it is clear that the near-singularity of these matrices, worsening as gate-open times decrease, represents a major practical difficulty in implementing Yen's method.

Alternative Algorithms

In light of the difficulty in matrix inversion which seems inherent in Yen's method, it is worthwhile to consider algorithms which are better adapted to the sampling required by the present work, i.e., very short gate-open periods. Yen's method apparently works best in the limit of long gate-open periods (approaching 100%), and this limit is the opposite of that toward which it is desirable to strive in the present case. It is potentially advantageous to adopt an algorithm which shows promise of applicability in the opposite limit, that of very short gate-open periods.

An example of a procedure which is somewhat better adapted than Yen's to the present situation is that of using pairs of sample data within gate-open windows. From these, mean and first-derivative values may be calculated. An existing explicit algorithm (Ref. 5) is then feasible for reconstructing signals from such signal values and first derivatives which are uniformly spaced in time.

Alternatively, pairs of sample data might be used to calculate means and first derivatives to which fictitious uniformly spaced "samples" could be fitted and processed. Again, for these pairs, an explicit algorithm which requires uniformly spaced rather than randomly spaced samples within each gate-open period is available (Ref. 5).

Unfortunately, the only evident alternatives are not likely to be useful if desirably high sampling rates are achieved. If more than a pair or perhaps three samples are acquired during single gate-open period, these explicit methods are apparently not applicable and no others are known. Still, it is just such high rates that would provide the greatest potential for determining unsteady velocity components at substantial multiples of the rotational frequency of the rotor, i.e., for high engine orders. Multiple samples per gate-open period increase the Nyquist frequency for the sampling to an equal multiple of one-half the rotational frequency. More than two or three samples per gate-open period are necessary in order to deal with unsteady components

much above the rotational frequency. Extension of the gated-LDA approach to measuring unsteady frequency components at the relatively high frequencies involved in multi-patch stall phenomena seems, therefore, unlikely.

ANALYTICAL/CFD MODEL OF CASCADES

Coupled with the experimental portion of the research there has been an effort to construct a tentative analytical model of the time-varying behavior of a cascade of airfoils. The approach has been to treat a cascade as a system of N interfering airfoils without any a priori assumptions concerning uniformity of loading from airfoil to airfoil. A search for other-than-uniform-flow solutions to the model equations should yield some insight into flow about highly loaded cascades.

Arbitrary Loading Cascade Model

The infinite two-dimensional cascade, obtained by unwrapping an annular cascade of differential radial extent, will have periodicity imposed over every N-bladed group of airfoils (Fig. 9). Here N represents the number of blades in the annular cascade from which the two-dimensional cascade was developed. Typically $10 < N < 100$ and is often chosen to be prime. For simplicity the airfoils are uncambered* and thin so that only the velocities normal to the chords need be considered in the boundary condition.

Under these proscriptions, including incompressibility of the fluid, the statement of the boundary conditions leads to a matrix expression of the following form

$$\begin{array}{c} m \backslash n \\ 1 \\ 2 \\ 3 \\ \\ N \end{array} \begin{array}{c} \begin{array}{cccc} 1 & 2 & 3 & N \end{array} \\ \begin{bmatrix} V_{11} & V_{12} & V_{13} \cdots\cdots & V_{1N} \\ V_{21} & V_{22} & V_{23} \cdots\cdots & V_{2N} \\ V_{31} & V_{32} & V_{33} \cdots\cdots & V_{3N} \\ \vdots & & & \vdots \\ V_{N1} & \cdots\cdots\cdots\cdots & & V_{NN} \end{bmatrix} \end{array} \begin{Bmatrix} \gamma_1(\xi) \\ \gamma_2(\xi) \\ \gamma_3(\xi) \\ \vdots \\ \gamma_N(\xi) \end{Bmatrix} = -V_m \begin{Bmatrix} 1 \\ 1 \\ 1 \\ \vdots \\ 1 \end{Bmatrix} - \sum_i \Gamma_i(\xi_i, \eta_i) \begin{Bmatrix} v_{1i}(x) \\ v_{2i}(x) \\ v_{3i}(x) \\ \vdots \\ v_{Ni}(x) \end{Bmatrix} \quad (1$$

*For lightly loaded, slightly cambered airfoils the idemvector on the RHS of Eq. (1) would be augmented by a function of x.

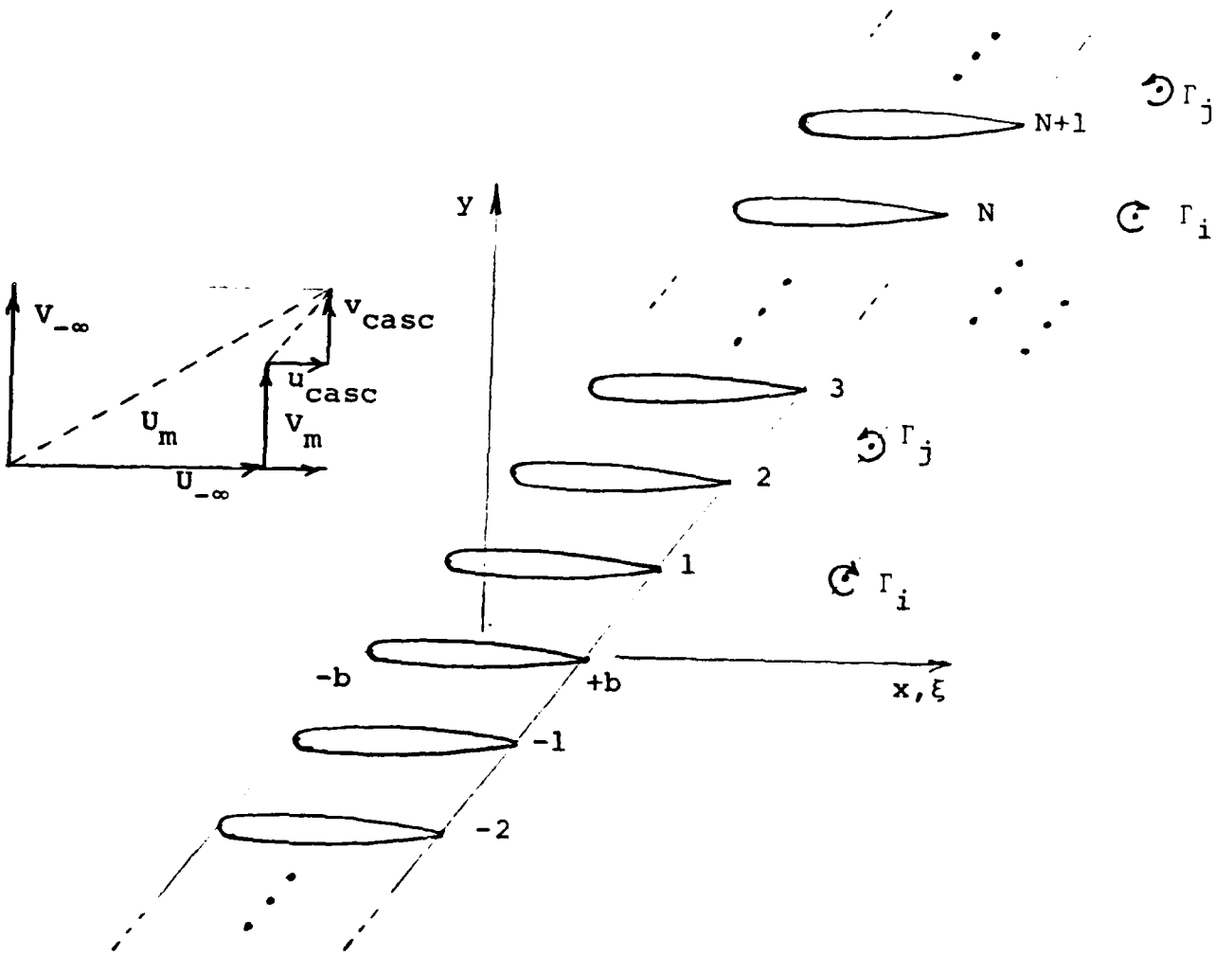

FIGURE 9: Geometry of infinite cascade derived from N-bladed annular cascade.

where V_{mn} are integral operators, V_{nn} are singular integral operators (i.e. on the main diagonal) and $\gamma_n(\xi)$ in the unknown vorticity, or distributed circulation, on the nth airfoil, $1 \leq n \leq N$. V_m is the component of the mean velocity normal to chordlines and is determined by specifying the (constant) vector velocity at upstream infinity and subtracting from it the velocity induced by all the vortices (both free and bound) in the field. In addition there are free vortices in the field. The ith free vortex of strength Γ_i and located at ξ_i, η_i and its N-spaced images induce the velocity, normal to the chord of the nth airfoil given by $\Gamma_i(\xi_i, \eta_i)v_{ni}(x)$.

The integral operators V_{mn}, accounting as they do for induction effects due to every Nth airfoil in an infinite array, are given by (see Fig. for the geometry of the cascade expressed in non-orthogonal coordinates).

$$V_{mn} = \int_{-b}^{b} (\text{———}) \; K_{mn}(x - \xi) \; d\xi \tag{2}$$

where

$$K_{mn} = \frac{1}{2\pi} \sum_{q=-\infty}^{\infty} \frac{\xi - x + (n-m+qN)s'}{[\xi - x + (n-m+qN)s']^2 + [n-m+qN)s'']^2} \tag{3}$$

$$s' = s \sin \beta, \qquad s'' = s \cos \beta \tag{4}$$

Thus, V_{mn} operates on γ_n to produce a contribution to the velocity at the mth blade.

Similarly, the velocities induced by the discrete vortices Γ_i are given by

$$v_{mi} = \frac{1}{2\pi} \sum_{q=-\infty}^{\infty} \frac{\xi_i - x + \eta_i \sin\beta - ms' + qNs'}{[\xi_i - x + \eta_i \sin\beta - (m-qN)s']^2 + [\eta_i \cos \beta - ms'' + qNs''} \tag{5}$$

Since there seems to be no direct method of manipulating the

matrix of operators, the equations are solved by assigning an expansion of aerodynamic modes to each vorticity distribution, say

$$\gamma_n(\xi) = A_n\left(\frac{1-\xi/b}{1+\xi/b}\right)^{\frac{1}{2}} + B_n\left(\frac{1+\xi/b}{1-\xi/b}\right)^{\frac{1}{2}} + D_n(1-\xi/b)^{\frac{1}{2}}\,(1+\xi/b)^{\frac{1}{2}} \qquad (6)$$

$$+ E_n\,\xi/b(1-\xi/b)^{\frac{1}{2}}\,(1+\xi/b)^{\frac{1}{2}},\ -b \leq \xi \leq b$$

then each Nth airfoil will have the same distribution, i.e.

$$\gamma_n = \gamma_{n+N} = \gamma_{n-N} = \gamma_{n+2N} \quad \text{etc.}$$

The coefficients A_n and B_n allow for singularities at the leading and trailing edges, respectively whilst D_n allows for an adjustment of the circulation. E_n provides for biasing the distribution more to the leading or trailing edges, depending on sign.

Then each integral is evaluated at a number of points, x, along the chord of each airfoil: four points in the case of the example expansion in Eq. (6). This is tantamount to satisfying the boundary conditions by collocation, so that with the current choice of 4 terms in Eq. (6), values of x = -b, -b/2, b/2, b would be appropriate.

With these definitions the equations are reduced to true matrix equations of order 4Nx4N (in this particular example).

$$[\alpha]\ \{A\} = -V_m\ \{1\} - \sum_i \Gamma_i\ \{v_i\} \qquad (7)$$

Here {A} is the column vector of unknown vorticity coefficients

$$\{A\} = [A_1,\ B_1,\ D_1,\ E_1,\ A_2,\ B_2,\ D_2,\ E_2,\ A_3, \ldots . D_{N-1},\ D_N]^T \qquad (8)$$

and V_m is a constant whose physical meaning has been described. In addition there may be a number of free vortices, Γ_i in the field, and their N-spaced images (see Fig. 1) which also induce the velocities expressed by

$$\Gamma_i(\xi_i,\eta_i)[v_{1i}(0),\ v_{1i}(1),\ v_{1i}(2),\ v_{1i}(3),\ v_{2i}(0),\ v_{2i}(1),\ldots v_{Ni}(3)]^T \tag{9}$$

Here ξ_i, η_i are the coordinates of the vortex of strength Γ_i.

The coefficient matrix $[\alpha]$ is of order 4NX4N and has the following general form

$$[\alpha] = \left[\begin{array}{ccccc|cccc}
\alpha^0_{11} & \beta^0_{11} & \delta^0_{11} & \varepsilon^0_{11} & \alpha^0_{12} & \beta^0_{12} & \delta^0_{12} & \varepsilon^0_{12}\cdots & \varepsilon^0_{1N} \\
\alpha^1_{11} & \beta^1_{11} & \delta^1_{11} & \varepsilon^1_{11} & \alpha^1_{12} & \beta^1_{12} & \delta^1_{12} & \varepsilon^1_{12}\cdots & \varepsilon^1_{1N} \\
\alpha^2_{11} & \beta^2_{11} & \delta^2_{11} & \varepsilon^2_{11} & \alpha^2_{12} & & & & \vdots \\
\alpha^3_{11} & \beta^3_{11} & \delta^3_{11} & \varepsilon^3_{11} & & & & & \vdots \\
\hline
\alpha^0_{21} & \beta^0_{21} & & & \alpha^0_{22} & \beta^0_{22} & & & \vdots \\
\alpha^1 & & & & & & & & \vdots \\
\vdots & & & & & & & & \vdots \\
\alpha^3_{N1} & \cdots & \cdots & \cdots & \cdots & \cdots & \cdots & \cdots & \varepsilon^3_{NN}
\end{array}\right] \tag{10}$$

The superscripts 0,1,2 and 3 refer to the collocation points chosen for satisfying the boundary conditions.

The coefficient matrix is the result of inserting Eqs. (6) and (3) into Eq. (2) and performing the indicated operation, e.g.

$$\beta^0_{12} = \int_{-b}^{b} \left(\frac{b+\xi}{b-\xi}\right)^{1/2} \frac{1}{2\pi} \sum_{q=-\infty}^{\infty} \frac{\xi - (-b/2) + (2-1+qN)s'}{[\xi-(-b/2) + (2-1+qN)s']^2 + [(2-1+qN)s'']^2} \tag{11}$$

Referring to Eq. (5), the velocity induced at x = -b/2 on airfoil n = 1 by the ith free vortex Γ_i is given by

$$v^0_{1i} = \Gamma_i \frac{1}{2\pi} \sum_{q=-\infty}^{\infty} \frac{\xi_i - (-b/2) + \eta_i \sin\beta - 1.s' + qNs'}{[\xi_i - (-b/2) + \eta_i \sin\beta - (m-qN)s']^2 + [\eta_i \cos\beta - (m-qN)s'']^2} \tag{12}$$

Nonuniform distribution which result from solving Eq. (7) for the vector {A} will depend critically on the field of free vortices $\sum_i \{\Gamma_i\}$.

Uniform Cascades as a Special Case

In the absence of free vortices, $\{\Gamma_i\} = \{0\}$, the solution of Eq. (7) will yield the typical result of uniform loading if there is imposed the same Kutta condition of smooth flow off the trailing edge of each blade. Setting all $B_n = 0$, so that the distributed circulation drops to zero at the trailing edge of every blade, results in more simultaneous equation than unknowns. Every 4th column, starting with the 2nd, (i.e., columns 2,6,10 etc.) may be eliminated since these terms always multiply a B_n component. Furthermore, the number of rows may also be reduced by one quarter by eliminating one of the collocation points, say $x = -b$, the leading edges of the foils.

It should be emphasized that these consequences of applying the Kutta condition are without mathematical foundation. This "condition" is an observable physical phenomenon which can be explained in the light of the slight, but nonvanishing, viscosity of the fluid. Thus, in any inviscid approximation to the flow such as the present one the Kutta condition becomes an arbitrary mathematical statement. The lesson to be learned from the consideration is that dynamic stalling of the cascaded airfoils cannot be determined entirely without the specification of analogous "Kutta conditions". When the passage flow reverses, smooth flow off the leading edges may be expected at certain times. If temporally separated flow

appears with separation streamline, emanating from leading and/or trailing edges, additional "separation conditions" may have to be imposed.

The partitioning of [α] from Eq. (9) into submatrices, of order 3x3, reveals certain symmetries when each submatrix is treated as an element, α_{mn}.

i) All elements on the main diagonal are equal, i.e. all α_{nn} are equal irrespective of n.

ii) All elements in a line parallel to the main diagonal are equal to each other, i.e. α_{mn} depends only on m-n and not on m and n individually. (Statement ii includes i).

iii) If m and n for one element are such that their difference is N greater or less than m-n for another element, the two terms are equal.

All these properties taken together are such that the matrix of subelements is a circulant matrix.

Provided that [α] is non-singular, this results in a solution to Eq. (1) in which all the A_n, D_n, E_n triplets are equal. The loading is the same on each airfoil. Since the loading is found to be uniform in this case, the a priori assumption that all the free vortices, Γ_i, are absent has been justified.

Nonuniform Solutions

Clearly, a preliminary estimate of nonuniform loading flow solutions may be synthesized by setting $A_n = 0$ for certain values of n and $B_n = 0$ for other values of n. Simultaneously it is necessary to eliminate the column in [α] associated with each

null coefficient. For every column eliminated it is also necessary to eliminate a row in order to maintain $[\alpha]$ as a square matrix. The resulting stall "patches" might then be expected to appear in the vicinity of those blades having $A_n = 0$.

This solution is somewhat unrealistic in the sense that there are no free vortices downstream of the cascade, nor do the stall patches propagate. These observations are tantamount to stating that the flow is steady in contradiction to what should be the physical reality.

More realistic solutions of the equations will depend upon the ability to link the temporal fluctuation in the $A_n(t)$, $B_n(t)$ and $D_n(t)$ to the strengths of the free vortices Γ_i and their trajectories. This is evident from the fact that the circulation around the nth airfoil is given by

$$\text{Circ}_n = \int_{-b}^{b} \gamma(\xi)\, d\xi = \pi b(A_n + B_n - 1/2\, D_n) \tag{13}$$

As the coefficients A_n, B_n and D_n change with time, the circulation changes and the shed circulation appears in the form of the free vortices in order to conserve the total circulation. Since the trajectory of each free vortex depends on time and on the flow velocity at the location of the vortex, it is clear that one method of obtaining the instantaneous field of velocities (and locus of vortices) is by a time-marching algorithm starting with some assumed initial configuration.

Although there are some avenues to be investigated in attempting to obtain the more realistic solutions, these have not been pursued up to the time of concluding this contract.

RESEARCH COMPRESSOR

This apparatus, constructed with ONR/NavAir funding, is a single stage axial flow compressor embodying a number of distinctive features. Some of these features are unique:

- Constant flow annulus has a 20 inch (0.508m) tip diameter and 12 inch (0.305m) hub diameter.
- Rotor drum is fitted with 36 uniform (chord 5.08cm and aspect ratio of 3) untwisted blades. Blades are shaft-mounted so that stagger may be changed by resetting a unison ring within the drum.
- Key housing sections are fabricated from polymethyl methacrylate (PMM) for ease of flow visualization. Housing sections designed for accepting LDA laser beams are of cast aluminimum with small PMM windows set in flush with the housing I.D.
- Inlet guide vanes and exit guide vanes (stator blades) are variable by means of unison rings and at design theoretically provide constant incidence on the rotor blades.
- Discharge throttle is followed by a large shipboard ventilation blower to allow adjustment of throughflow independently of compressor speed.
- Variable speed drive is provided by a 20 h.p. (14.9 kW) D.C. motor with solid state controller and feedback tachometer driving through a belted pulley system.
- Intake is conventional bellmouth and nose bullet with four front main bearing support struts.

The compressor has been entirely assembled and run at a number of speeds to calibrate the controller/tachometer. Rotor blade setting was at 45 degrees, exit guide waves were at design.

Since delays with the laboratory program had prevented the procurement of any LDA data on the compressor directly, some rudimentary measurements were made using alternative instrumentation in the last few weeks of the contractual period.

At the nominal setting of the inlet guide vanes, the midradius blade angle is zero. Various rotor speeds and throttle settings were used in the first tests using a wedge probe to determine the velocity triangles entering the rotor at this reference radius. At combinations of speed and throttle where the rotor incidence was in excess of about 11 deg. it was found that the flow was increasingly unsteady and accompanied by an audible change in the acoustic "signature". The presumption that the propagating stall was present was provisionally confirmed with a small linen thread tuft in the flow which became increasing agitated as the incidence increased above about 11 deg. (It was the objective of the entire research program to replace such provisional and qualitative observations by quantitative in-rotor determinations of the unsteady velocity field).

Additional tests with the fan on or off, and with different settings of the inlet guide vanes (from -9° to 15° from nominal) confirmed that rotating stall was present when the incidence, or rotor blade loading, was increased above some critical value. Two additional observations were also possible in the limited final testing under the contract: (1) the region of large incidence and large flow fluctuations (the stall patches) appeared first and were most intense at the rotor blade tips, and (2) negative axial flow

components (i.e. upstream flow) were detected near the outer housing under the most severe conditions of stalling.

With these intriguing clues at hand the experiments were necessarily terminated awaiting further means of possible continuation.

CONCLUSIONS

The work leading up to this final report has been focussed primarily on the empirical mapping of the unsteady flow field in the rotor passages of an axial flow compressor (single stage). Although this experimental result was not finally achieved within the contract time limit, several important conclusions were reached in relation to the data acquisition system, the data processing algorithms, the analytical/CFD modeling of compressor stall and the research compressor itself.

Design of the data acquisition system was governed by the presumed necessity of following the evolution of the stall process within a single (the same) blade passage. With the fixed LDV this implied that velocity realizations could be obtained only during a small fraction of each rotor revolution. Hence the data sample on which a spectral analysis could be performed was extremely sparse, the more so since each passage width had to be subdivided into a number of still smaller intervals (windows). In order to characterize the unsteady velocity distribution at least ten and probably 20 or 30 subdivisions will be required. Microprocessor-based hardware and software have been developed that will theoretically accept this quality of data and output the desired unsteady flow field information. Simulations have demonstrated this conclusion.

Seeding of the compressor flow to increase the data rate will be required. Some studies reported herein have indicated, provided the carrier gas and free stream velocities are fairly well-matched, that the seeding can be accomplished and will produce

the desired result. A residual concern is the health hazard or the particular seeding material that is to be used. A tentative candidate material is glycerine.

These preliminary results having to do with the LDA measurements have led to the major conclusion that the experimental data, and its spectral analysis, should henceforth be based on more than one (preferably all) of the flow passages. Hence the emphasis should shift from gating, per se, to an accurate time/space location of any and all velocity realizations that are obtained. The microprocessor data reduction algorithm will then be based on the presumed identity, albeit shifted in time, of the processes in all the blade passages.

The flow modelling initiated toward the end of the contract period was sufficient to demonstrate that a nonuniform distribution of cascade loading, including local regions of reverse flow, is possible and satisfies all the governing boundary conditions. Questions of flow stability and rate of propagation of the non-uniformity (stall patches) cannot be settled without augmenting the model. In the future, it will be necessary to add a field of free vorticity, in addition to the bound vorticity studied here, in order to predict stability and compute propagation rates. The method for doing this will involve the application of the Random Vortex Method, or a similarly-based algorithm, to the flow near and downstream of the cascade. It should also be possible to qualify or validate the model on a linear cascade of limited extent, or possibly a stationary annular cascade. However, the single-stage

axial-flow research compressor and LDA development should continue for ultimate corroboration of the results in a more realistic, engine-like geometry.

The eventual, long-term objective is to be able to predict the number of stall zones, and their tangential rate of propagation, for application to axial compressors and fans. This information is critical for the prediction of blade resonance in rotating stall, for the prediction of the inception of stall flutter and possibly also for the description of compressor surge. If these goals can be attained, they will represent the first instances in which the phenomena were accurately described on the basis of unsteady cascade aerodynamics rather than stage characteristics.

REFERENCES

1. Sisto, F., "Research on the Behavior of Cascaded Airfoils Under Conditions of High Mean Loading and Flow Unsteadiness," Final Technical Report on contract Nooo14-79-C-0765 NR-094-391, Stevens Institute of Technology, 30 June 1982.

2. Dring, R.P., "Sizing Criteria for Laser Anemometry Particles", J. of Fluids Engineering (ASME), Vol. 104, March 1982, pp. 15-17.

3. Abramovich, G.N., The Theory of Turbulent Jets, M.I.T. Press, Cambridge (1963), Chapt. 5.

4. Yen, T.L., "On Non-Uniform Sampling of Bandwidth-Limited Signals", IRE Trans. Grant Dreory, Vol. CT-3, Dec. 1956, pp. 251-257.

5. Papoulis, A., Signal Analysis, McGraw-Hill, N.Y. (1977), pp. 191-196.

UNCLASSIFIED

SECURITY CLASSIFICATION OF THIS PAGE (When Data Entered)

REPORT DOCUMENTATION PAGE		READ INSTRUCTIONS BEFORE COMPLETING FORM
1. REPORT NUMBER ME-RT-83007	2. GOVT ACCESSION NO. AD-A139799	3. RECIPIENT'S CATALOG NUMBER
4. TITLE (and Subtitle) Behavior of Cascaded Rotor Airfoils Under Conditions of High Mean Loading and Flow Unsteadiness		5. TYPE OF REPORT & PERIOD COVERED Final Technical Report for period 6/1/83-5/31/83 6. PERFORMING ORG. REPORT NUMBER
7. AUTHOR(s)		8. CONTRACT OR GRANT NUMBER(s) N00014-82-K-0369
9. PERFORMING ORGANIZATION NAME AND ADDRESS Mechanical Engineering Department Stevens Institute of Technology Hoboken, New Jersey 07030		10. PROGRAM ELEMENT, PROJECT, TASK AREA & WORK UNIT NUMBERS NR094-419
11. CONTROLLING OFFICE NAME AND ADDRESS Office of Naval Research 1800 N. Quincy Street Arlington, VA 22217		12. REPORT DATE 15 August 1983 13. NUMBER OF PAGES 41
14. MONITORING AGENCY NAME & ADDRESS(if different from Controlling Office) See above		15. SECURITY CLASS. (of this report) Unclassified 15a. DECLASSIFICATION/DOWNGRADING SCHEDULE

16. DISTRIBUTION STATEMENT (of this Report)

Approved for Public Release Distribution Unlimited

17. DISTRIBUTION STATEMENT (of the abstract entered in Block 20, if different from Report)

See above

18. SUPPLEMENTARY NOTES

19. KEY WORDS (Continue on reverse side if necessary and identify by block number)

Unsteady Flow, Compressor Stall, Propagating Stall, Rotating Stall, Laser Doppler Anemometer, Laser Doppler Velocimeter

20. ABSTRACT (Continue on reverse side if necessary and identify by block number)

The objectives of this research program were to measure the unsteady flow field in the rotor passage of an axial compressor and map this velocity field when operating near rotor blade stall. A laser doppler velocimeter system was developed for this purpose and used in conjunction with a single stage compressor designed expressly to facilitate these measurements. An extensive data acquisition system utilizing microcomputer components was designed

DD FORM 1 JAN 73 1473 EDITION OF 1 NOV 65 IS OBSOLETE
S/N 0102-014-6601

UNCLASSIFIED

SECURITY CLASSIFICATION OF THIS PAGE (When Data Entered)

and partially assembled and data processing algorithms were developed to yield the velocity mapping from the data.

Various program sub-elements were completed, but a successful on-rotor velocity realization was not achieved at contract termination. Propagating stall was observed on the compressor and modelling studies using simulated inputs to the data processing system indicated a potential for successful unsteady velocity field mapping.

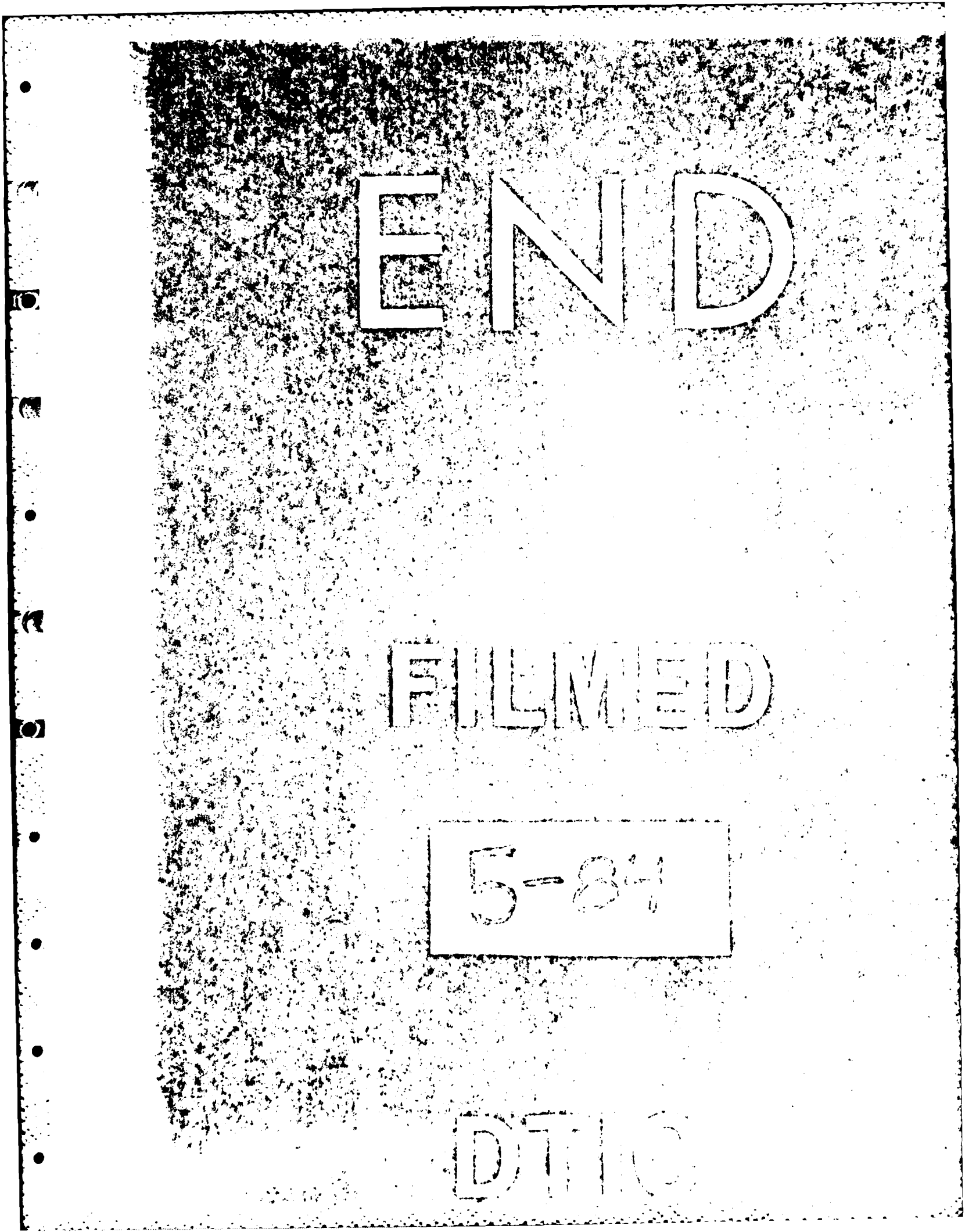
END
FILMED
5-84
DTIC